Materials and Structures (2016) 49:3445–3457
DOI 10.1617/s11527-015-0731-2

ORIGINAL ARTICLE

An accelerated sulfate resistance test for concrete

Roman Loser · Andreas Leemann

Received: 6 May 2015 / Accepted: 5 October 2015 / Published online: 13 October 2015

Abstract The sulfate resistance of concrete was tested using drying-immersion cycles of varying duration in different sulfate solutions. The measured expansion in the different protocols showed a correlation to the sulfate profiles in the test specimens determined by EDX. Based on the magnitude of expansion and the test duration, a suitable protocol for testing job-site concrete was identified. A matrix of 20 concrete mixtures was tested with this protocol. The test permitted to distinguish the effect of cement type, w/c and paste volume on expansion. Measurements of the dynamic E-modulus made it possible to link expansion and mechanical damage and to define a limit value for expansion. As this test appears to be suitable to determine the potential of concrete for expansion induced by ettringite formation due to sulfate ingress, it was introduced into the Swiss norms.

Keywords Concrete · Sulfate attack · Expansion · Acceleration · Test

R. Loser · A. Leemann (✉)
Empa - Swiss Federal Laboratories for Materials Science and Technology, Dübendorf, Switzerland
e-mail: andreas.leemann@empa.ch

1 Introduction

In external sulfate attack, sulfate-bearing water interacts with concrete, leading to its degradation. While this is a widely studied reaction in cement and concrete research, only few studies characterizing sulfate attack on real structures have been published [e.g. 1–9]. The majority of studies about sulfate attack are based on tests in the laboratory [e.g. 10–16]. Testing the sulfate resistance of cement paste, mortar and concrete usually involves the immersion of specimens in sulfate solution allowing its ingress by diffusion. The disadvantage of such an approach is a typical test durations of several months up to a few years. The determined parameters are generally length and mass change complemented with a visual assessment and, in the case of research, often with microstructural analysis. These tests are mainly suited to study the mechanisms of sulfate attack under such conditions and the cement-specific sulfate resistance. However, the construction industry needs a method with a relatively short duration to test the sulfate resistance of specific concrete mixtures produced with different cement types, mineral additions and w/c. Based on the results mix designs are developed to decrease the probability of damages to a given structure in the future. In addition, such a test has to be used to control concrete production. As external sulfate attack is a common phenomenon in Alpine tunnels [11, 13–16], the need for a test method meeting

these needs was obvious. In connection with the two Alptransit tunnel projects in Switzerland an accelerated test using four drying-immersion cycles (2 days drying, 5 days immersion) to accelerate sulfate ingress was developed [17]. After its introduction to the standards and use for a few years, a research project identified the limits of the method [18]. The main problem with the method was the low expansion of the cores making a distinction between different concrete mixtures difficult. This low expansion was mainly a result of the short duration of immersion (four times 5 days). Although the method succeeded in accelerating the sulfate ingress, the short duration of immersion (no additional immersion after drying-immersion cycles) limited the amount of the expansive phases formed [18, 19].

This paper presents the results of the experimental program conducted to improve the mentioned method to reach a higher expansion of the test specimens allowing a more reliable distinction between different concrete mixtures. It had to be taken into account that the test duration was not prolonged significantly making it unsuitable for controlling concrete production. First, the duration of the drying and immersion cycles is varied to study its effect on sulfate ingress. Sulfate solutions of different composition are used to determine their impact on expansion. Measurements of the dynamic E-modulus are performed on selected mixtures to follow the physical degradation accompanying the length changes. Additionally, the sulfate ingress and the mineral assemblages are investigated with scanning electron microscopy (SEM) combined with energy dispersive X-ray spectroscopy (EDX). Based on the results, a final protocol is defined and for validation a set of 20 concrete mixtures produced with five different cements is tested.

2 Materials and methods

2.1 Materials

Two ordinary Portland cements (EN 197-1: CEM I 32.5 R and CEM I 42.5 N HS), a cement containing 15 mass% limestone powder (EN 197-1: CEM II/A-LL 42.5 N), a cement containing approximately 15 mass% of limestone powder and 20 mass% low-calcium fly ash (EN 197-1: CEM II/B-M (V-LL) 32.5 R) and a ground granulated blast-furnace slag cement (EN 197-1: CEM III/B 32.5 N HS) were used to produce the concretes. The composition of the five cement types used is given in Table 1. The maximum grain size of the alluvial gravel aggregates was 22 mm except for the mixture with the added letter S (self-compacting concrete with maximum grain size of 16 mm). The aggregates consist of a mixture of limestone, siliceous limestone, sandstone and minor amounts of dolomite and gneiss. The mix design of the concrete is given in Table 2. The experimental matrix was designed in a way that a clear distinction between the effect of w/c, cement type and paste volume should be possible.

The specimens (cubes $150 \times 150 \times 150$ mm^3) were stored at 20 °C and 90 % relative humidity for 24 h after production. Afterwards, they were demolded and stored again in the same climate.

The cubes for testing compressive strength were kept in these conditions until 28 days. For the other methods cores were taken from cubes at the age of 26 days. Eight cores with a diameter of 28 mm and a length of 148 mm were taken for testing sulfate resistance (six for length measurements and two for measurements of the dynamic E-modulus) and three cores with a diameter of 100 mm and a length of 50 mm for measuring oxygen. Afterwards, the cores were again stored at 20 °C and 90 % relative humidity until reaching an age of 28 days.

The cores for the determination of oxygen diffusion coefficient were conditioned at 20 °C and 35 RH for seven days and then dried in an oven at 50 °C for another 7 days before the measurement started (age of 42 days).

2.2 Methods

2.2.1 General concrete properties

Concrete flow was measured according to EN 12350-5 and air void content according to EN 12350-7. Compressive strength of the concrete cubes was determined according to EN 12390-3.

The oxygen diffusion coefficient D_O was measured as described in [20–22] on three cores (diameter of 100 mm, height of 50 mm). An oxygen flow was applied on one side of the cores and a nitrogen flow on the other side. The gas pressure on both sides of the cores was identical. The oxygen content in the nitrogen flow was measured until equilibrium was

Table 1 Composition of the cements

Cement	Abbreviation used for concrete	CaO	SiO_2	Al_2O_3	Fe_2O_3	MgO	K_2O	Na_2O	SO_3	LOI
CEM I 32.5 R	OPC	64.1	20.7	4.7	3.0	2.2	0.9	0.2	2.4	0.9
CEM I 42.5 R HS	OPC-HS	59.3	19.2	3.4	5.4	4.0	0.7	0.3	3.2	3.8
CEM II/A-LL 42.5 N	L	61.0	17.8	4.3	2.7	1.7	1.0	0.2	2.8	7.8
CEM II/B-M 32.5 R	L-FA	52.3	23.6	6.9	3.8	1.7	1.2	0.3	2.5	6.9
CEM III/B 32.5 N HS	SL	46.4	30.1	10.0	1.3	5.2	0.7	0.4	4.1	1.1

LOI loss on ignition

Table 2 Mix design of the concrete

Concrete/cement (–)	Aggregate (kg/m^3)	$m_{s/g}$ (–)	Cement (kg/m^3)	Water (kg/m^3)	w/c (–)	Addition (kg/m^3)	Paste volume (l/m^3)
OPC-45	1929	0.54	335	150	0.45	1.3SP	257
OPC-50	1929	0.54	315	157	0.50	0.3SP	257
OPC-60	1931	0.54	280	168	0.60	–	257
OPC-45H	1799	0.54	400	180	0.45	–	307
OPC-45S	1680	1.00	450	200	0.45	1.8SP + 1.1VMA	343
OPC-HS-45	1927	0.54	335	150	0.45	1.3SP	257
OPC-HS-50	1927	0.54	315	157	0.50	0.6SP	257
OPC-HS-60	1929	0.54	280	168	0.60	–	257
OPC-HS-45S	1678	1.00	450	200	0.45	2.3SP + 1.1VMA	343
L-45	1930	0.54	330	148	0.45	0.7SP	257
L-50	1931	0.54	310	155	0.50	0.3SP	257
L-60	1923	0.54	280	168	0.60	–	257
L-45S	1679	1.00	445	197	0.45	1.8SP + 1.1VMA	343
L-FA-45	1924	0.54	325	146	0.45	1.0SP	257
L-FA-50	1927	0.54	305	152	0.50	0.3SP	257
L-FA-60	1922	0.54	275	165	0.60	–	257
L-FA-45S	1677	1.00	435	193	0.45	2.2SP +1.1VMA	343
SL-45	1928	0.54	325	146	0.45	1.3SP	257
SL-50	1930	0.54	305	152	0.50	0.6SP	257
SL-60	1925	0.54	275	165	0.60	–	257
SL-45H	1794	0.54	390	174	0.45	–	307
SL-45S	1672	1.00	440	195	0.45	1.8SP + 1.1VMA	343

$m_{s/g}$ mass ratio between sand and gravel, *SP* polycarboxylate-based superplaticizer, *VMA* viscisity modifying agent

reached. Afterwards, the oxygen diffusion coefficient was calculated according to [20].

The dynamic E-modulus of the cores was measured using an Elastometer LABEK. Two cores of selected concrete mixtures were measured at different stages of sulfate resistance test: before the test, after the drying and immersion cycles at the end of the test.

After measuring dynamic E-modulus, specimens for microstructural analysis were prepared of the same cores. A disc was cut from the middle part of the cores, dried in an oven at 50 °C for 3 days, impregnated with epoxy resin, polished and coated with carbon. The analysis was conducted with an environmental scanning electron microscope (ESEM-FEG XL30). The

samples were studied in the high vacuum mode (2.0–6.0 × 10^{-6} Torr) with an accelerating voltage of 15 kV and a beam current of 170–190 μA. The sulfur concentration was determined with energy dispersive X-ray spectroscopy (EDX). An EDAX 194 UTW detector, a Philips digital controller and Genesis Spectrum Software (Version 4.6.1) with ZAF corrections was used. At each depth analysed (1.0, 3.5, 7.0, 10.5, 14 mm for the sulfur profiles and additionally at 0.2 and 2.2 mm for the phase assemblages), two or three line scans were made, totalling 80 point measurements per depth. The elements Na, Mg, Al, Si, S, K, Ca and Fe were analysed.

2.2.2 *Sulfate resistance*

On the cores used to determine sulfate resistance (six cores per series) a plug gauge for strain measurements was glued at their ends. Four cycles of drying and immersion were applied after the concrete reached an age of 28 days in all protocols (row "conditioning" in Table 3). The duration of the drying during drying-immersion was either 2, 5 or 12 days according to the different protocols (Table 3). Drying was conducted in a well ventilated oven at 50 °C (protocol 7: 40 °C) with a distance between single cores ≥25 mm. The cores do not reach constant mass during drying as shown in [18]. However, the temperature was not further increased to minimize the loss of chemically bound water in the cement hydrates and to avoid drying damage of the concrete. After removing the cores from the oven, they were stored in a desiccator at 20 °C for 1 h. The majority of cores showed no efflorescence on their surface. Some cores showed minor efflorescence limited to two or three locations per core along the interface between aggregates and cement paste extending a few millimetres. The salt solutions with concentrations given in Table 3 were prepared from deionised water. The ratio of sulfate solution to volume of specimen was set to 4.5 and the solution was not exchanged during the test in all protocols. The temperature of the solutions was 20 °C during the entire test. The containers containing solution and cores were covered with a lid to prevent evaporation and as a result to prevent changes in salt concentration. The duration of the immersion during drying-immersion was either 2 or 5 days according to the different protocols (Table 3). After the conditioning (drying-immersion cycles), the samples were stored in the specific solutions for another 8 weeks for all protocols. This is in contrast to SN 505262/1:2003, where no additional immersion is used. The goal of the drying-immersion cycles was to accelerate sulfate ingress, while the additional immersion allows more time for the formation of expansive phases. As a result higher expansion is reached enabling a better distinction between the sulfate resistance of different concrete mixtures. Length and mass changes of the cores during the drying-immersion cycles and the additional immersion were recorded (mean of six cores per concrete and solution). During the drying-immersion cycles length measurements were always conducted after immersion. While the cores took up a total between 193 and 420 kg/m^3 of solution when immersed after drying (sum of the four cycles/Table 4), their weight remained nearly constant

Table 3 Conditioning (always four cycles of drying and immersion) and solutions used in the protocols 1–7 ($MgSO_4$/Na_2SO_4 solution with mass-ratio = 1/9)

N°	Conditioning		Solutions for immersion			
	Drying (days)	Immersion (days)	Na_2SO_4 34 g/l SO_4^{2-}	Na_2SO_4, 68 g/l SO_4^{2-}	$MgSO_4$, 34 g/l SO_4^{2-}	$MgSO_4$/Na_2SO_4, 34 g/l SO_4^{2-}
1	2 (50 °C)	5 (20 °C)	X	–	–	–
2	5 (50 °C)	2 (20 °C)	X	–	–	–
3	5 (50 °C)	2 (20 °C)	–	X	–	–
4	5 (50 °C)	2 (20 °C)	–	–	X	–
5	5 (50 °C)	2 (20 °C)	–	–	–	X
6	12 (50 °C)	2 (20 °C)	X	–	–	–
7	12 (40 °C)	2 (20 °C)	X	–	–	–

Table 4 Properties of the concrete mixtures including mass and length change during the sulfate resistance test (protocol 2)

Concrete/cement	w/c (–)	Flow (cm)	Air void content (%)	$f_{c,28}$ (MPa)	D_O (10^{-8} m/s^2)	Δm (kg/m^3)	Δl (‰)
OPC-45	0.45	59	1.5	56.3	0.87	260	0.977
OPC-50	0.50	51	1.8	45.8	1.22	296	2.209
OPC-60	0.60	52	1.1	38.9	1.76	362	6.765
OPC-45H	0.45	62	1.2	46.6	1.47	340	2.257
OPC-45S	0.45	70	1.6	55.5	0.84	342	3.155
OPC-HS-45	0.45	42	1.9	58.7	1.24	279	0.279
OPC-HS-50	0.50	46	1.7	47.2	2.26	358	0.401
OPC-HS-60	0.60	49	0.9	34.0	4.03	394	0.292
OPC-HS-45S	0.45	50	3.8	56.7	1.51	403	0.345
L-45	0.45	42	1.8	49.7	0.97	320	3.446
L-50	0.50	50	1.7	42.4	1.38	347	7.322
L-60	0.60	56	0.8	33.2	2.37	402	5.983
L-45S	0.45	55	2.6	51.7	1.17	415	8.855
L-FA-45	0.45	49	1.5	44.3	1.20	305	0.674
L-FA-50	0.50	48	1.3	38.2	1.57	341	1.936
L-FA-60	0.60	54	0.8	28.2	3.01	420	16.446
L-FA-45S	0.45	66	2.3	46.3	1.69	403	1.221
SL-45	0.45	45	2.2	56.2	0.21	193	0.233
SL-50	0.50	43	1.6	43.3	0.62	239	0.297
SL-60	0.60	46	1.4	33.0	0.78	297	0.422
SL-45H	0.45	43	2.0	47.2	0.47	262	0.412
SL-45S	0.45	53	2.8	57.9	0.32	254	0.258

$f_{c,28}$, cube compressive strength after 28 days; D_O, oxygen diffusion coefficient; Δm, total uptake of sulfate solution during the four drying and immersion cycles (protocol 2); Δl, expansion during additional storage of 8 weeks (protocol 2)

during the additional immersion of 8 weeks. The mass changes during the entire test served as control parameter.

In phase 1 the effect of the seven different protocols on expansion was investigated. The conditioning in protocol 1 corresponds to the one of SN 505262/1:2003. The increased duration of drying in protocols 2–7 was used to increase sulfate uptake of the cores during immersion. Doubling the sulfate concentration of the solution in protocol 3 had the same goal. $MgSO_4$ in the sulfate solution was used in protocols 4 and 5 to investigate its effect on expansion. It is reported in literature that the effect of $MgSO_4$ differs from the one of Na_2SO_4 and that these differences can be cement-specific [23–25]. A limited set of four different concrete mixtures were tested in phase 1. Two mixtures with CEM I and a w/c of 0.45 and 0.60 (mixture OPC-45 and OPC-60 in Table 2) were used to investigate the effects of the varying drying and solutions in all protocols (1–7). Two additional concrete mixtures produced with CEM III/B and a w/c of 0.45 and a w/c of 0.60 (mixture SL-45 and SL-60 in Table 2) were only exposed to protocols 2, 4 and 5 (Table 3). These four concrete mixtures were chosen for phase 1 as they encompass the entire range of w/c and cement clinker content of the test matrix (Table 2).

In phase 2 the concrete mixtures shown in Table 2 were tested using protocol 2. Protocol 2 was chosen based on the analysis of phase 1.

3 Results and discussion

3.1 Concrete properties

A summary of the concrete properties and results of the sulfate resistance test (protocol 2) are shown in

Table 4. Within one cement type compressive strength increases and oxygen diffusion coefficient decreases with decreasing w/c. At identical w/c concrete OPC, OPC-HS and SL display a higher compressive strength than concrete L and in particular concrete L-FA. Concrete SL exhibits by far the lowest oxygen diffusion coefficient D_O while the values of concrete OPC-HS are the highest. Sulfate uptake during immersion in protocol 2 increases with increasing w/c and paste volume. The differences between the different cement types are small with the exception of concrete SL that shows a lower sulfate uptake. The expansion is discussed in detail in the following paragraphs.

3.2 Phase 1

3.2.1 Expansion

Changing from 2 days drying and 5 days immersion (protocol 1) to 5 days drying and 2 days immersion (protocol 2) increases expansion during the additional immersion (Fig. 1; Table 5). Extending drying to 12 days (protocols 6 and 7) increases expansion further, independently of the drying temperature. Doubling the Na_2SO_4 concentration has little effect on expansion (protocol 3). Using $MgSO_4$ instead of Na_2SO_4 (protocol 4) leads to a significant decrease in expansion. The decrease is less pronounced in the mixed $MgSO_4$/Na_2SO_4 solution (protocol 5). This applies to concrete OPC and to concrete SL.

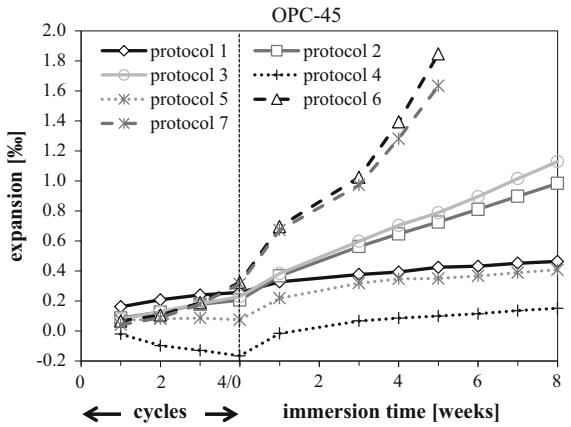

Fig. 1 Expansion of the concrete OPC-45 with varying drying-immersion cycles in different solutions. 0–4 = cycles during conditioning, 4–12 weeks of additional immersion

Table 5 Expansion of the concrete exposed to varying conditioning and sulfate solutions in the protocols 1–7

N°	OPC-45 (‰)	OPC-60 (‰)	SL-45 (‰)	SL-60 (‰)
1	0.26/0.46	0.34/0.71	0.27/0.54	0.89/1.46
2	0.21/0.98	0.29/7.54	–	–
3	0.23/1.13	0.43/6.64	–	–
4	−0.17/0.15	−0.14/0.18	−0.16/0.15	0.10/1.14
5	0.08/0.41	0.18/1.78	0.13/0.36	0.73/1.38
6	0.33/1.85 (5)	0.54/7.15 (5)	–	–
7	0.31/1.63 (5)	0.57/7.60 (5)	–	

The first number represents the expansion after the four drying-immersion cycles and the second one the total expansion after the additional immersion of 8 weeks. (5) indicates that cores of these concrete mixtures had only 5 weeks of additional immersion instead of 8

3.2.2 Sulfur profiles

The sulfur profiles after the conditioning of the concrete mixtures OPC-45 and OPC-60 shows a decrease of the sulfur content with increasing depth (Fig. 2a). Prolonging the drying and shortening the immersion from protocol 1 to protocol 2 results in an increased sulfur penetration of the cores. Concrete OPC-45 exhibits a lower sulfur content in both protocols than concrete OPC-60. The sulfur profiles in the cores changes only insignificantly during the additional immersion after the conditioning. Doubling the Na_2SO_4 concentration in the solution (protocol 3) only slightly changes the sulfur profile (Fig. 2b). In the centre of the cores the concentrations are higher compared to protocol 2, but at the edge they are lower. However, the use of $MgSO_4$ solution (protocol 4) leads to significantly lower sulfate ingress (Fig. 2b). The samples in this solution exhibit a brucite layer on the surface (Fig. 3). The use of the mixed $MgSO_4$ + Na_2SO_4 solution results in higher sulfate ingress compared to protocol 4 but to a lower one compared to protocol 2 (Fig. 2b).

3.2.3 Discussion of phase 1

All changes of protocol 1 lead to higher expansions, if Na_2SO_4 solution is used. Although the sulfur profiles exhibit a certain scatter due to the small area measured, they clearly indicate the reasons for differences in expansion: the longer drying increases the

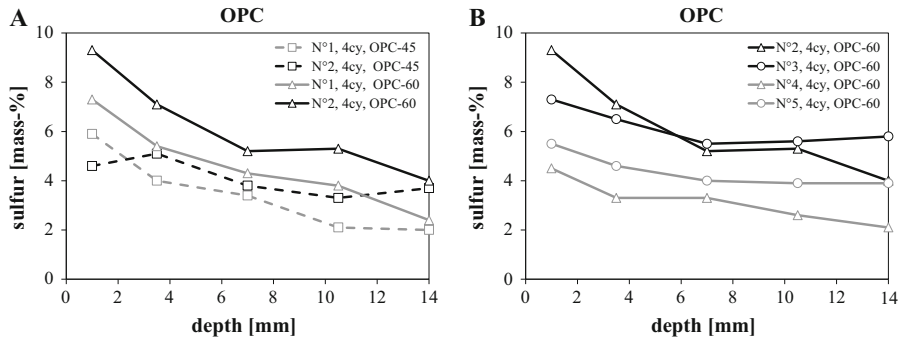

Fig. 2 **a** Sulfur profiles in the cores of concrete OPC-45 and OPC-60 after the conditioning according to protocols 1 and 2, **b** sulfur profiles in the cores of concrete OPC-60 after the conditioning according to protocols 2, 3, 4 and 5 (different sulfate solutions)

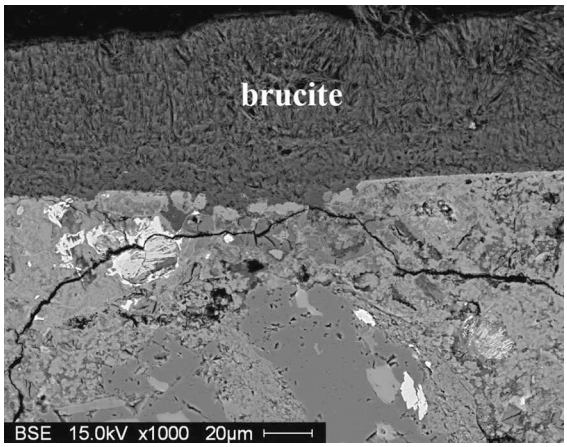

Fig. 3 Formation of brucite on the surface of concrete core OPC-60 tested according to protocol 4 ($MgSO_4$-solution)

capacity for sulfate uptake by capillary suction. As the concrete with the lower w/c dries slower, its sulfur uptake is consequently smaller compared to the concrete with the higher w/c. This directly translates into a lower expansion. Although the cores do not take up sulfur in the additional immersion, they still expand considerably (Fig. 1). This seems to be a kinetic effect. The expansive phases do not have sufficient time to form during the short immersion (4 × 2 days) in the conditioning. As such, the potential of the ingressed sulfate to form expansive phases is not exploited. However, the additional immersion allows their formation and results in additional expansion. The lower expansion of the cores immersed in solutions containing $MgSO_4$ goes together with a lower amount of sulfate ingressing the cores (Fig. 2b). This seems to be the result of the continuous brucite layer forming on the surface of the cores (Fig. 3). Brucite formation was observed in other studies as well [23, 24, 26]. Obviously, the brucite layer hinders sulfate ingress.

Based on these results a revised test procedure can be defined. First, the change of the duration of drying and immersion cycles compared to protocol 1 makes sense as it results in higher expansions during additional immersion. Although drying for 12 days either at 50 or at 40 °C leads to the highest expansions (protocols 6 and 7), the prolongation of the test duration is a disadvantage. Additionally, already the expansions achieved in protocols 2 and 3 enable a good distinction between the different concrete mixtures. As the SO_4^{2-} concentration in protocol 3 is very high with 68 g/l and does not result in a higher expansion compared to protocol 2, it is not considered. Due to the problem of brucite formation hindering sulfate ingress, the use of solutions containing $MgSO_4$ is discarded (protocols 4 and 5). This leaves protocol 2 as the most suitable for the defined goals. The duration of the test of 12 weeks is still regarded as acceptable to meet the demands of the concrete producers in regard to duration. Consequently, the concrete mixtures shown in Table 2 are tested using protocol 2 and their results are presented in the following paragraph. Only the length changes after the conditioning (during additional immersion) are used to assess the sulfate resistance, because effects of drying on the length changes can be excluded. Protocol 2 is now published in the SN 505262/1:2013 [27].

3.3 Phase 2

3.3.1 Expansion and dynamic E-modulus

The expansion of concrete OPC-45, OPC-50 and OPC-60, all of them having an identical volume of

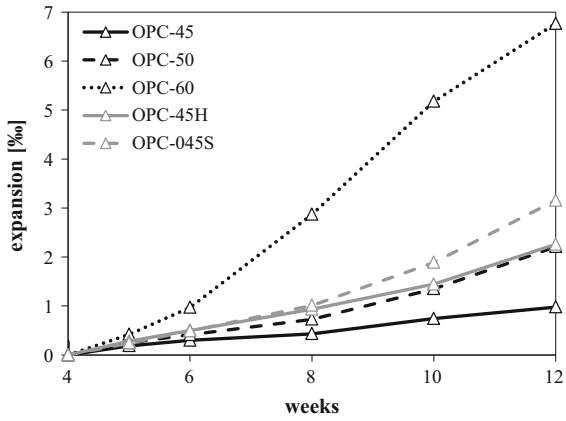

Fig. 4 Expansion during additional immersion of concrete OPC versus time (protocol 2)

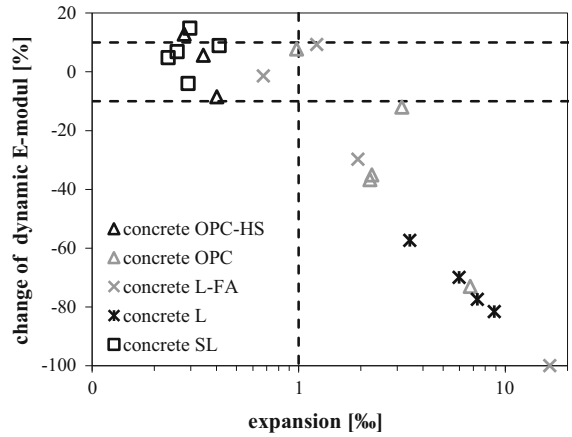

Fig. 6 Change of dynamic E-modulus as a function of expansion during additional immersion

paste, increases with increasing w/c (Fig. 4). The same applies to the corresponding mixtures of concrete L, L-FA and SL (Fig. 5a). An exception is concrete L-60 that shows a lower expansion as concrete L-50 (Fig. 5a). Its expansion gradient considerably decreases in the last 4 weeks of immersion. The total expansion and the differences in expansion of concrete OPC-HS are very low. Therefore, there is no recognizable trend caused by w/c. As such, the measured expansions show a clear connection to the used cement type. The expansion decreases going from concrete L to concrete OPC to concrete L-FA (Fig. 5a). Concrete mixtures SL and OPC-HS both exhibit very low expansion levels.

Increasing the cement paste volume from 255 to 345 l/m^3 at a constant w/c of 0.45 leads to a marked increase in expansion in the case of concrete OPC and L and to a small one of concrete L-FA (Fig. 5b). The very low expansion values of concrete OPC-HS and concrete SL do not increase by the increased paste volume.

Dynamic E-modulus of the concrete is mainly dependent on w/c and is in the range of 35 to 45 GPa before the test. Some concrete mixtures with low expansion show an increase of dynamic E-modulus up to 15 % likely caused by ongoing cement hydration (Fig. 6). All concrete mixtures showing a relative decrease of dynamic E-modulus larger than 10 % during additional immersion exhibit an expansion larger than 1 ‰. Only concrete L-FA-45S expands more than 1 ‰ and does not show a decrease of E-modulus.

3.4 Elemental profiles and mineral assemblages

Concrete mixtures OPC-45, OPC-60, SL-45 and SL-60 are used to compare sulfur ingress, mineral

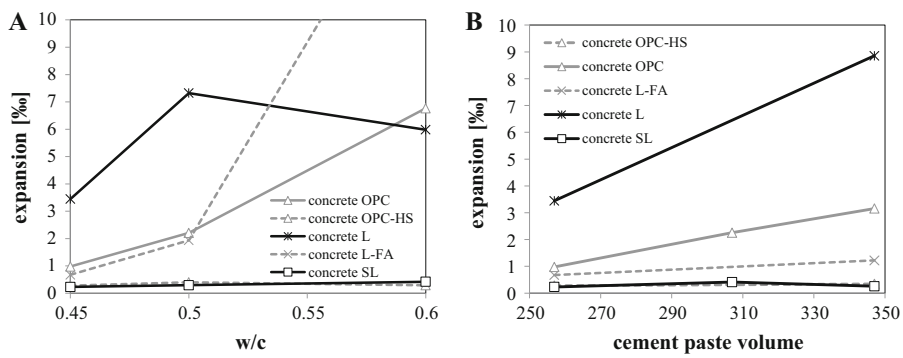

Fig. 5 **a** Expansion during additional immersion versus *w/c* of concrete produced with different cement types (expansion of concrete L-FA-60 = 16.4 ‰/protocol 2) and **b** expansion after additional immersion of 8 weeks versus cement paste volume (concrete *w/c* of 0.45/protocol 2)

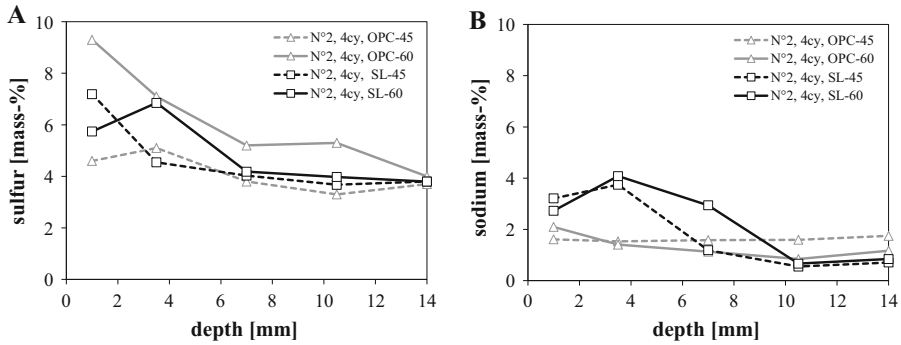

Fig. 7 Sulfur (**a**) and sodium (**b**) content versus depth of the concrete mixtures OPC-45, OPC-60, SL-45 and SL-60 after 4 drying-immersion cycles (cy)

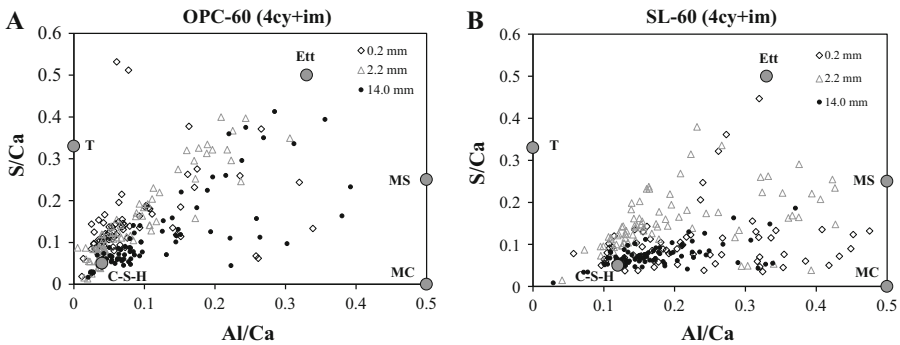

Fig. 8 S/Ca-ratio versus Al/Ca-ratio in concrete mixtures OPC-60 (**a**) and SL-60 (**b**) after the additional immersion at a depth of 0.2, 2.2 and 14.0 mm (*T* thaumasite, *C–S–H* calcium–silicate–hydrate, *Ett* ettringite, *MS* monosulfate, *MC* monocarbonate). The mean value of C–S–H in concrete SL is placed at a higher Al/Ca-ratio compared to concrete OPC due to the higher aluminum content of the cement

assemblages and microstructure as they represent the entire range in regard to w/c and clinker content.

The sulfur content in concrete OPC-60 is higher than in concrete OPC-45 except in the middle of the core (Fig. 7). The differences in the sulfur content of concrete SL-45 and SL-60 are not significant. The depth reached by the sulfate seems to be higher in concrete SL-60 as indicated by the sulfur concentration at a depth of 3.5 mm. The sodium content in concrete OPC-45 and OPC-60 are between 1 and 2 mass%. Compared to the middle of the core concrete SL-45 has an increased sodium content up to a depth of 3.5 mm and SL-60 up to a depth of 7 mm. The increased sodium content reaches a greater depth than the increased sulfur content.

The mineral assemblages present in the concrete produced with w/c 0.45 and 0.60 are principally the same but are present at a different depth in agreement with the sulfur profiles. As a simplification, only the mineral assemblage of the concrete OPC-60 and SL-60 are described here (Fig. 8).

In the core of sample OPC-60, monosulfate and ettringite are present beside some portlandite and the main hydrate phase calcium-silicate-hydrate (C–S–H). In a depth of 10.5, 7.0, 3.5 mm the same mineral assemblage is found but with an ongoing increase towards the surface of the sample in the number of points indicating ettringite. Moving even further towards the surface three things happen: the amount of monosulfate is decreasing, the amount of ettringite is increasing and the S/Ca-ratio of C–S–H is increasing. Additionally, there are some points at a depth of 0.2 mm indicating the presence of gypsum (S/Ca = 1.0, Al/Ca = 0). In this area, the Ca/Si-ratio is slightly decreased (not shown).

In the centre of concrete SL-60 monocarbonate, monosulfate and C–S–H are present. At a depth of 10.5 and 7.0, monocarbonate starts to decrease and the

S/Ca-ratio of the C–S–H starts to increase. This increase keeps on to a depth of 1.0 mm. At 3.5 mm from the surface ettringite appears with increasing occurrence up to a depth of 1.0 mm. At 0.2 mm ettringite is nearly absent, no monosulfate is present and the Al/Ca-ratio of the C–S–H increases significantly, while its Si/Ca-ratio decreases (not shown).

4 Discussion of phase 2

The measured concrete expansion is a combined effect between the diffusivity (Table 4) of the samples and their cement mineralogy. First, a concrete of low diffusivity loses less water during drying and consequently takes up less sulfate solution by capillary suction during immersion. Secondly, the amount of ettringite formed and with it the resulting expansion is dependent on the amount of aluminium available for its formation.

The samples with low w/c have a higher clinker content and with it a higher theoretical potential for expansion. However, the relation between expansion and w/c clearly shows that a low diffusivity limiting sulfate ingress is more important than the theoretical expansion potential.

The used cement type has a clear effect on the resulting expansion. Although concrete OPC has a higher clinker content than concrete L, the expansion is slightly lower most likely due to its lower diffusivity. The expansion of concrete L-FA is even lower due to its further reduced clinker content. In spite of its high diffusivity the expansion of concrete OPC-HS is very low as a result of its low calcium-aluminate content. The low expansion of concrete SL can be attributed both to its low diffusivity and its cement mineralogy. The amount of sulfate ingressing the concrete is relatively low. Although its high aluminum content would result in a high amount of monosulfate and monocarbonate during hydration, the low degree of hydration of the slowly reacting slag is expected to limit the available amount of aluminum for ettringite formation. Additionally, the low Ca/Si-ratio of the hydrates makes the occurrence of supersaturation as a needed prerequisite for expansive ettringite formation less likely [28].

Concrete OPC, L and L-FA that show high expansions at high w/c exhibit an increasing expansion with increasing paste volume. This effect can be attributed to two effects. On the one hand side, the volume of the material that can expand increases with increasing paste volume. On the other hand, the volume of aggregates that exert a restrain on the concrete expansion decreases.

Based on the identification of the mineral assemblages in different depths of the cores the reactions of the hydrates with sulfate are comparable in concrete OPC and SL; monocarbonate and monosulfate are converted to ettringite. In both systems the increasing occurrence of points indicating ettringite goes together with an increase in sulfur content. However, in order to exert stress by crystallization pressure, ettringite has to form in the condition of supersaturation [29]. As already mentioned, this situation is less likely in concrete SL-60 than in concrete OPC-60 due to lower supersaturation of the pore solution with respect to ettringite at lower Ca/Si ratios of the C–S–H [28]. Gypsum is only found in minor amounts close to the surface of concrete OPC-60. However, its formation is not likely to have an effect on expansion. But its presence indicates supersaturation of the sulfate in the pore solution [28, 29]. Based on thermodynamic modelling, gypsum starts to form at a sulfur content in the cement paste of about 20 mass% [30]. This value is not reached on average in these samples. Due to an inhomogeneous sulfur distribution, occasional presence of gypsum seems still possible locally. The shift to a higher S/Ca-ratio observed in the C-S–H upon sulfate ingress into the cores goes together with the conversion of finely distributed monocarbonate/monosulfate within the C–S–H to ettringite leading to crystallisation pressure in small pores as postulated by Chen et al. [31, 32]. This seems to be confirmed by the change in pore size distribution linked to the formation of ettringite in mortars exposed to sulfate solution [33]. Moreover, the observed changes in mineral assemblages of the studied concrete mixtures agree with thermodynamic modelling [25, 30, 34]. The sequence of the identified phase assemblages in relation to the sulfur concentration in the concrete is comparable to the one found in structures exposed to sulfate attack [9, 11, 16] and to the one present in mortar used for long-term immersion tests [30–36]. As such this accelerated test seems to be an applicable approach to determine the resistance of concrete to expansion caused by ettringite formation. Due to the relative short test duration it is not able to assess the resistance to thaumasite

formation whose kinetics is considerably slower than the one of ettringite. It can be expected that the effect of w/c on thaumasite resistance is similar to its effect on ettringite formation as it governs sulfate ingress. However, as the availability of calcium and carbonate plays a crucial role in thaumasite formation, the ranking between the different cements can be expected to be different than observed here.

Porous materials can be seriously damaged during drying-immersion cycles in Na_2SO_4 solution due to thenardite/mirabilite formation, as tests on sandstone have shown [37–39]. If mirabilite forms under conditions of supersaturation, the resulting crystallisation pressure should be able to damage concrete [38]. However, in these experiments with sandstone at least six drying-immersion cycles with a considerably higher concentrated Na_2SO_4 solution (108 g SO_4^{2-}/l) than in this study were needed to cause damage due to mirabilite formation. Still mirabilite formation has to be taken into consideration when testing concrete with drying-immersion cycles. Thenardite would form during the drying stage and mirabilite with the potential of damaging the concrete at the beginning of the immersion stage. In [38] the damage occurred within an immersion time of 6 h. Consequently, damage due to thenardite/mirbilite formation would be expected during the drying-immersion cycles. However, the expansion mainly takes place during the additional immersion of 8 weeks in the sulfate resistance test. Still, the sodium levels of all samples are increased when compared to the composition of the cements. Obviously, sodium is able to penetrate the entire sample during the test. In spite of this increase, the sodium concentration in concrete OPC-60 is fairly low, making thenardite/mirabilite formation unlikely. The sodium concentration in the slag-system is higher. However, the maximum concentration of sodium does not go together with the maximum of sulfur concentration. As sodium has to be bound to another counter-ion than sulfate, the probability of thenardite formation seems to be low. During the additional immersion sodium concentration is decreasing as it is highly soluble and therefore diffuses into the sulfate solution to reach equilibrium. The used sulfate concentration in combination with the applied number of drying-immersion cycles, the main expansion during the additional immersion and not during drying-immersion cycles, the microstructural evidence and the identified phases cannot completely exclude thenardite/mirabilite formation, but make damage related to it highly unlikely.

In sulfate attack not only the volume change is of importance but degradation of the mechanical concrete properties as well. The measurements of the dynamic E-modulus enables to link both parameters. The decrease of E-modulus observed in some of the mixtures of concrete SL seems to be related to minor damages caused by drying [40]. However, the relation between change of E-modulus and length change during immersion enables to specify a limit value of expansion. As concrete with an expansion lower than 1 ‰, shows a relative decrease of dynamic E-modulus below 10 %, an expansion below 1 ‰ seems a suitable value to distinguish concrete with high sulfate resistance form one with low sulfate resistance.

5 Repeatability and comparability

Although some information about repeatability of protocol 2 could be given based on the performed tests, the most appropriate way to assess repeatability and comparability is a Round Robin test. Shortly after protocol 2 was published in the Swiss standard SN 505262/1:2013, such a Round Robin was performed with a total of 13 participating Swiss labs, accredited according to ISO 17025 [VAB, 41]. Because the protocol was new, the participating laboratories had little experience with it. Four different concrete mixtures were tested. Every lab performed two tests per concrete (repeatability). Mean length change during additional immersion (average of six cores), repeatability and comparability are presented in Table 6. It has to be noted that in spite of the small core diameter of 28 mm and a maximum grain size of the aggregates in the concrete mixtures of normally 32 mm (8 mm for mixture 2), the scatter between the six cores tested per series was relatively low (Table 6) without single cores as outliers.

6 Conclusions

In a first phase of the study the effect of varying drying-immersion cycles and sulfate solutions on the length change and the sulfate ingress into concrete was studied. In the second phase concrete produced with five different cement types was tested with the protocol identified as the most suitable one. In addition to length

Table 6 Results of a Round Robin test using protocol 2

Concrete mixture	1	2	3	4
Number of labs taken into account	9	13	11	10
Mean of length change (‰)	0.251	0.629	0.538	5.574
Variation coefficient of the six cores per series (%)	18.7	13.3	16.7	22.8
Variation coefficient repeatability (%)	6.8	4.0	11.7	9.0
Var iation coefficient comparability (%)	32.1	16.2	21.2	40.0

measurements, the dynamic E-modulus was determined and the microstructure including the composition of the mineral assemblages was investigated.

Based on measured expansions and the sulfur profiles the following conclusion can be drawn for phase 1:

- Changing the drying-immersion cycles from 2/5 to 5/2 days leads to higher sulfate ingress in the cores.
- Doubling the concentration of the sodium sulfate solution to 68 g/l of SO_4^{2-} does not increase expansion.
- The use of magnesium sulfate results in a decreased sulfate ingress due to the formation of brucite on the concrete surface partly sealing the cores.
- Prolonging the drying step from 5 to 10 days increases the sulfate uptake of the cores but leads to an increased test duration.
- Four drying-immersion cycles (5/2 days) in a sodium sulfate solution (34 g/l of SO_4^{2-}) followed by an immersion for 8 weeks (protocol 2) is regarded as best balance between sulfate ingress, expansion and test duration.

The following can be concluded applying protocol 2 for testing the different concrete mixtures:

- The test is able to distinguish concrete produced with different cement types, w/c and paste volumes.
- The expansion in the test is strongly dependent on the cement type used. Concrete OPC-HS and SL expand little, while an increasing expansion is observed going from concrete L-FA to concrete OPC and concrete L.
- Expansion of concrete L-FA, OPC and L increases with increasing w/c and increasing paste volume.
- A decrease of dynamic E-modulus is observed when concrete reaches an expansion above 1 ‰ during the additional immersion.
- EDX point analysis on concrete OPC and SL indicate that expansion can be attributed to the phase conversion from monocarbonate/monosulfate to ettringite.
- The sulfur content in the paste and the formed mineral assemblages are comparable with the ones in on-site concrete exposed to sulfate attack and mortar used in long-term immersion tests.

It is a matter of fact that external sulfate attack on concrete structures is more complex that any lab test is able to imitate. Concrete structures under sulfate attack are damaged by expansion due to ettringite formation, strength loss due to thaumasite formation often combined with leaching, stress caused by salt crystallisation or a combination of these phenomena. The presented test gives an indication about the potential of concrete damages due to ettringite formation. Due to its relatively short duration and its sensitivity to w/c, cement type and paste volume it is suited to survey the production of sulfate resistant concrete in concrete plants.

Acknowledgments The Swiss Federal Road Office is acknowledged for financing this study, P. Lura for critically reviewing the manuscript.

References

1. St John DA (1982) An unusual case of ground water sulfate attack on concrete. Cem Concr Res 12:633–639
2. Diamond S, Lee RJ (1999) Microstructural alterations associated with sulfate attack in permeable concretes. Materials science of concrete: sulfate attack mechanisms. American Ceramic Society, Westerville, pp 123–173
3. Sahu S, Badger S, Thaulow N (2002) Evidence of thaumasite formation in Southern California concrete. Cem Concr Compos 24:379–384
4. Leemann A, Loser R (2011) Analysis of concrete in a vertical ventilation shaft exposed to sulfate-containing groundwater for 45 years. Cem Concr Compos 33:74–83
5. Bellmann F, Erfurt W, Ludwig HM (2012) Field performance of concrete exposed to sulphate and low pH

conditions from natural and industrial sources. Cem Concr Compos 34:86–93
6. Mittermayr F, Baldermann A, Kurta C, Rinder T, Klammer D, Leis A, Tritthart J, Dietzel M (2013) Evaporation—a key mechanism for the thaumasite form of sulfate attack. Cem Concr Res 49:55–64
7. Mittermayr F, Bauer C, Klammer D, Böttcher ME, Leis A, Escher P, Dietzel M (2012) Concrete under sulphate attack: an isotope study on sulphur sources. Isot Environ Healt Stud 48:105–117
8. Romer M, Holzer L, Pfiffner M (2003) Swiss tunnel structures: concrete damage by formation of thaumasite. Cem Concr Compos 25:1111–1117
9. Pfiffner M, Holzer L (2001) Schädigungsmechanismen der Betonkorrosion in Tunnelbauwerken. Bundesamt für Strassen, ASTRA Report 1999/145, Bern (**in German**)
10. Thorvaldson T (1952) Chemical aspects of the durability of cement products. In: Proceedings of the 3rd international symposium on chemistry of cement, London, pp 436–465
11. Marchand J, Skalny J (1999) Sulfate attack mechanism. Am Ceram Soc, Westerville, pp 123–174
12. Skalny J, Marchand J, Odler I (2002) Sulfate attack on concrete. Spon Press, London
13. Nehdi ML, Suleiman AR, Soliman AM (2014) Investigation of concrete exposed to dual sulfate attack. Cem Concr Res 64:42–53
14. Abubaker F, Lynsdale C, Cripps J (2014) Investigation of concrete–clay interaction with regards to the thaumasite form of sulfate attack. Constr Build Mater Int Conf Sustain Constr Mater Technol 67A:88–94
15. Peyvandi A, Holmes D, Soroushian P, Balachandra AM (2014) Monitoring of sulfate attack in concrete by ^{27}Al and ^{29}Si MAS NMR spectroscopy. J Mater Civil Eng. doi:10.1061/(ASCE)MT.1943-5533.0001175
16. Bentz DP, Davis JM, Peltz MA, Snyder KA (2014) Influence of internal curing and viscosity modifiers on resistance to sulfate attack. Mater Struct 47:581–589
17. SN 505262/1 (2003) Beton—Ergänzende Eigenschaften (available in German and French)
18. Loser R, Leemann A, Niederhauser, R (2011) Prüfung des Sulfatwiderstandes von Beton nach SIA 262/1, Anhang D: Anwendbarkeit und Relevanz für die Praxis. ASTRA Forschungsbericht Nr. 1355, Bern (**in German**)
19. Leemann A, Loser R (2012) Accelerated sulfate resistance test for concrete—chemical and microstructural aspects. In: Second international conference on microstructural-related durability of cementitious composites, Amsterdam, paper 141
20. Lawrence CD (1984) Transport of oxygen through concrete. In: Glasser FP (ed) The chemistry and chemically-related properties of cement, vol 35. British Ceramic Society, London, pp 277–293
21. Buenfeld NR, Okundi E (1998) Effect of cement content on transport in concrete. Mag Concr Res 50:339–351
22. Villani C, Loser R, West MJ, Di Bella C, Lura P, Weiss JW (2014) An inter lab comparison of gas transport testing procedures: oxygen permeability and oxygen diffusivity. Cem Concr Compos 53:357–366
23. Gollop RS, Taylor HFW (1995) Microstructural and microanalytical studies of sulfate attack III. Sulfate-resisting Portland cement: reactions with sodium and magnesium sulfate solutions. Cem Concr Res 25:1581–1590
24. Gollop RS, Taylor HFW (1996) Microstructural and microanalytical studies of sulfate attack. IV. Reactions of a slag cement paste with sodium and magnesium sulfate solutions. Cem Concr Res 26:1013–1028
25. Al-Amoudi OSB, Maslehuddin M, Saadi MM (1995) Effect of magnesium sulfate and sodium sulfate on the durability performance of plain and blended cements. ACI Mater J 92:15–24
26. Kunther W, Lothenbach B, Scrivener KL (2013) On the relevance of volume increase for the length changes of mortar bars in sulfate solutions. Cem Concr Res 46:23–29
27. SN 505262/1 (2013) Beton—Ergänzende Eigenschaften, (**available in German and French**)
28. Kunther W, Lothenbach B, Skibsted J (2015) Influence of the Ca/Si ratio of the C-S-H phase on the interaction with sulfate ions and its impact on the ettringite crystallization pressure. Cem Concr Res 69:37–49
29. Flatt RJ, Scherer GW (2008) Thermodynamics of crystallization stresses in DEF. Cem Concr Res 38:325–336
30. Schmidt T, Lothenbach B, Romer M, Neuenschwander J, Scrivener KL (2009) Physical and microstructural aspects of sulfate attack on ordinary and limestone blended Portland cements. Cem Concr Res 39:1111–1121
31. Yu C, Sun W, Scrivener K (2015) Degradation mechanism of slag blended mortars immersed in sodium sulfate solution. Cem Concr Res 72:37–47
32. Yu C, Sun W, Scrivener K (2013) Mechanism of expansion of mortars immersed in sodium sulfate solutions. Cem Concr Res 43:105–111
33. Müllauer W, Beddoe RE, Heinz D (2013) Sulfate attack expansion mechanisms. Cem Concr Res 52:208–215
34. Lothenbach B, Bary B, Le Bescop P, Schmidt T, Leterrier N (2010) Sulfate ingress in Portland cement. Cem Concr Res 40:1211–1225
35. Gollop RS, Taylor HFW (1992) Microstructural and microanalytical studies of sulfate attack. I. Ordinary Portland cement paste. Cem Concr Res 22:1027–1038
36. Kunther W, Lothenbach B, Scrivener K (2013) Influence of bicarbonate ions on the deterioration of mortar bars in sulfate solutions. Cem Concr Res 44:77–86
37. Flatt RJ (2002) Salt damage in porous materials: how high supersaturations are generated. J Cryst Growth 242:435–454
38. Tsui N, Flatt RJ, Scherer GW (2003) Crystallization damage by sodium sulphate. J Cult Herit 4:109–115
39. Angeli M, Hébert R, Menéndez B, David C, Bigas JP (2010) Influence of temperature and salt concentration on the salt weathering of a sedimentary stone with sodium sulphate. Eng Geol 115:193–199
40. Loser R, Leemann A (2011) Sulfatwiderstand von Beton: verbessertes Verfahren basierend auf der Prüfung nach SIA 262/1, Anhang D. ASTRA Report FGU 2010/001, Bern (**in German**)
41. Report Nr. 2-1-039-06.14b (2014) VAB-Ringversuch Sulfatwiderstand von Beton nach SIA 262/1, Anhang D (**in German**)